Detailed urban object-based classifications from WorldView-2 imagery and LiDAR data: supervised vs. fuzzy rule-based

Alireza Hamedianfar[1]

Assoc. Prof. Dr.Helmi Zulhaidi Mohd Shafri[1,2]

Prof. Dr. Shattri Mansor[1,2]

Assoc.Prof. Dr. Noordin Ahmad[3]

[1]Department of Civil Engineering, Faculty of Engineering, Universiti Putra Malaysia(UPM)

[2]Geospatial Information Science Research Centre (GISRC), Faculty of Engineering,Universiti Putra Malaysia (UPM)

[3]National Space Agency, Bangunan Komersil PJH, 62570 Putrajaya, Malaysia

hzms04@gmail.com

ali.hamedianfar@gmail.com

Commission 3

Introduction

Content

- ❑Introduction
- ❑ Objectives
- ❑ Study area
- ❑Methodology
- ❑ Results and Discussions
- ❑Conclusion

Introduction

Urbanization Phenomenon:

- **Growth of built-up area and man-made structures**
- **Rapid transformation of natural environment to Impervious Surfaces (IS)**
- **IS distribution as a major contributor to urbanization and environmental condition (Arnold & Gibbons, 1996; Weng 2012).**
- **Roofs as the 25% coverage of urban areas (Akbari et al. 2003)**

Introduction

Roofing materials:

- **Concrete tile**
- **Clay tile**
- **Metal**
- **Asbestos**
- **Polycarbonate**

How roofing materials can affect environmental condition and quality?

- **Pollution**
- **Health**
- **Heat/energy**

Introduction

Pollution:

Roof runoff as a source of **water pollution** (Ballo et al. 2009)

Factors affecting surface water quality (Göbel et al. 2007; Gikas and Tsihrintzis 2012):

- **Roofing materials**
  Heavy metals such as zinc, copper and cadmium have been reported to be a source of contamination for surface water (Van Metre and Mahler 2003).

Other factors

- Conditions and slope of roofs
- Differences in usage of buildings (e.g. residential or industrial)

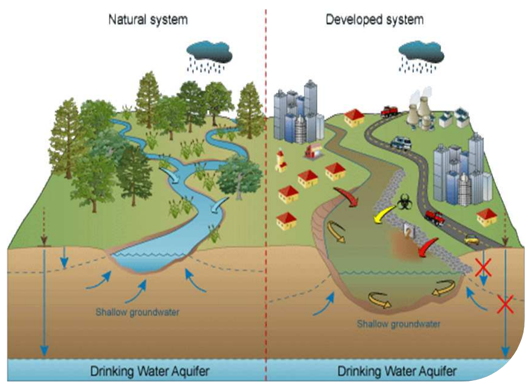

Introduction

Health:

Asbestos roofs as contributor to Lung Cancer

- In 2004 , 107,000 deaths and 1,523,000 Disability Adjusted Life Years (DALYs) (Frassy et al 2012)
- *Asbestos roofs* marketing and use was banned in **European Union** on January 1, 2005 (following the directive 76/769/CEE) (Frassy et al 2012).
- A consensus was achieved on banning of asbestos by **Department of Occupational Safety and Health (DOSH)** on 28 March 2011 in **Malaysia** (Safitri et al 2013).
- Complete ban in Malaysia is under negotiation and process (Safitri et al 2013).

Introduction

✓ **How we can get information about roof material types in large study area?**

1- Field visit, but

- too labor intensive
- very time consuming for large study area.

2- Hyperspectral Remote sensing offer great potential to map surface materials, but

- Provides limited coverage
- too expensive

3- New generation of Very High Resolution (VHR) satellite imagery

- WorldView-2 image
- much more efficient and cost effective

Current trends with land cover classification

Classification Approach	Advantage	Disadvantage
spectral-based Image analysis	✓ Sufficient for medium spatial multispectral image and hyperspectral imagery (Weng 2007; Envi-zoom tutorial 2010)	o Only based on pixel-values (DNs). o Poor performance in handling VHR imagery. o Not able to utilize spatial and textural information (Blaschke and Strobl, 2001; Myint et al. 2011).
Object-based image analysis (OBIA) **1-Supervised** **2-Rule-based**	✓ Change the classification element to image object. ✓ Utilization of all spatial, spectral, and textural information. ✓ Able to provide advanced rule-sets to map different target (Myint et al. 2011; Bhaskaran et al. 2012; Hamedianfar and Shafri 2013).	o Often results in unclassfied and mixed objects when dealing with intra-urban targets (Pinho et al 2012, Hamedianfar and Shafri 2013)

Objectives

- To identify optimal object-based rule-sets for roof material detection and other urban features
- To provide cartographically pleasing outline of roof infrastructure by using LiDAR and very high spatial resolution imagery of WorldView-2
- To compare the accuracy and efficiency of rule-based classifier and supervised SVM classifier in utilizing of **LiDAR** and **WorldView-2 image**

Study area and data

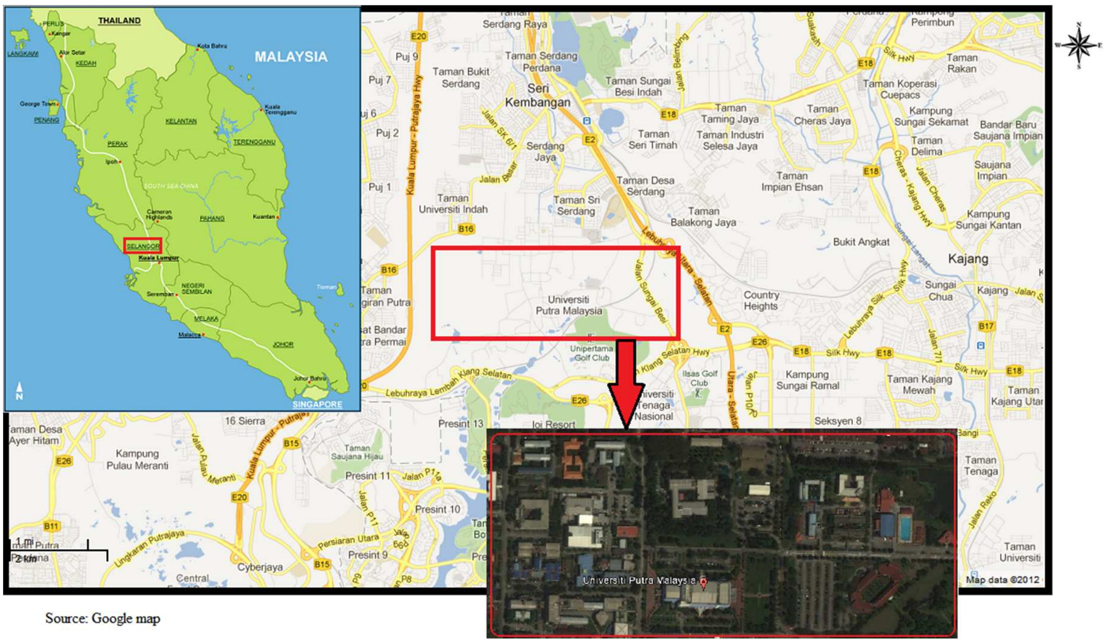

Source: Google map

XXV International Federation of Surveyors Congress, Kuala Lumpur, Malaysia, 16 – 21 June 2014

Data for this research rely on World-view2 (WV-2) imagery. WV-2 sensor includes:

- Panchromatic channel(0.5m spatial resolution)
- Eight multispectral channels(1.8m spatial resolution)

Band	Spectral Range
1	Coastal: 400 - 450 nm
2	Blue: 450 - 510 nm
3	Green: 510 - 580 nm
4	Yellow: 585 - 625 nm
5	Red: 630 - 690 nm
6	Red Edge: 705 - 745 nm
7	Near-IR1: 770 - 895 nm
8	Near-IR2: 860 - 1040 nm

Sensor bands of WorldView-2, 8-band multispectral images

LiDAR (Light Detection and Ranging) data

LiDAR is an active remote sensing technology that measures distance with reflected laser light (Jensen 2005)

3D view

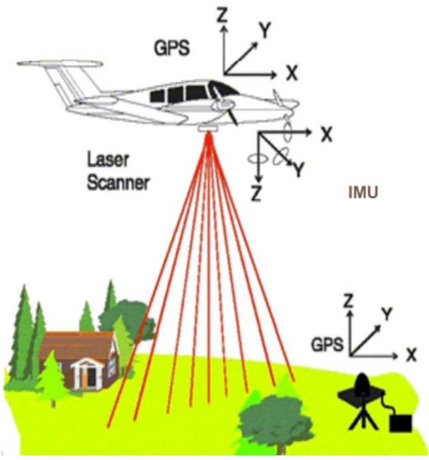

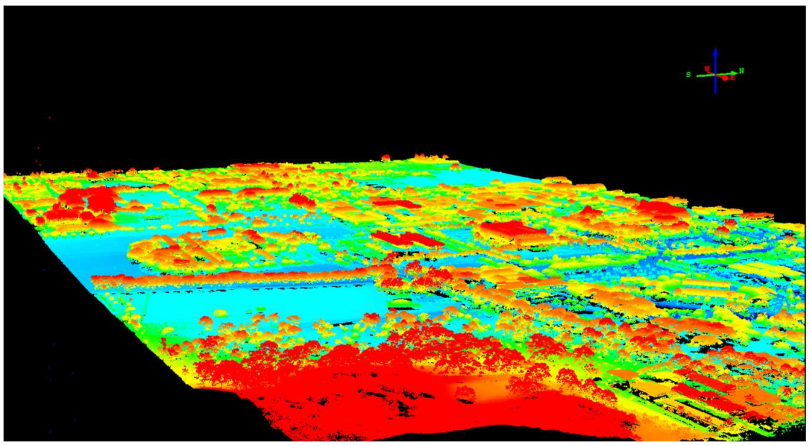

LiDAR (Light Detection and Ranging) data

2D view

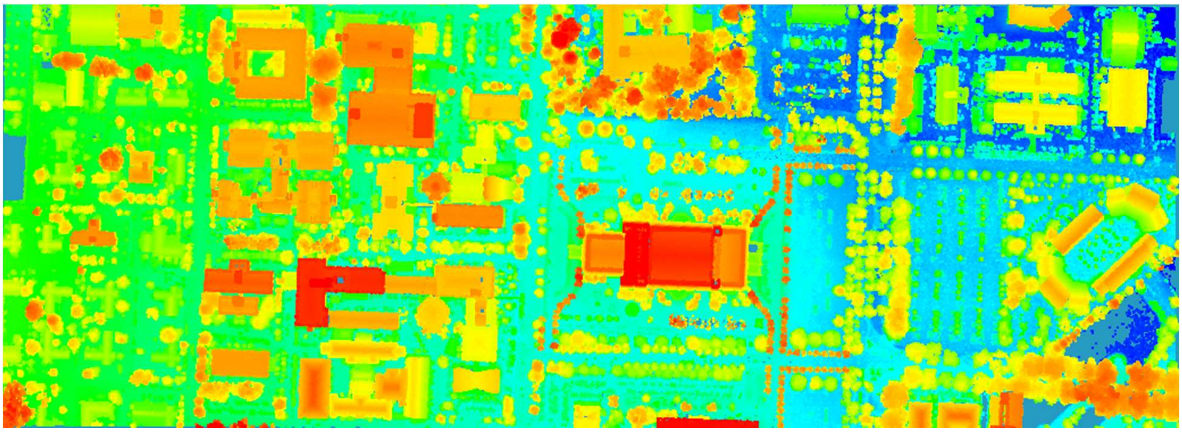

- Ancillary data : LiDAR products (DSM, DEM, nDSM[1])

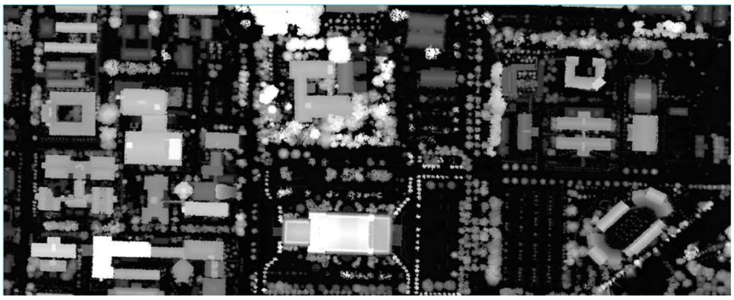

nDSM image

WorldView-2 image

[1]nDSM = Normalized Digital Surface Model

XXV International Federation of Surveyors Congress, Kuala Lumpur, Malaysia, 16 – 21 June 2014

Methodology

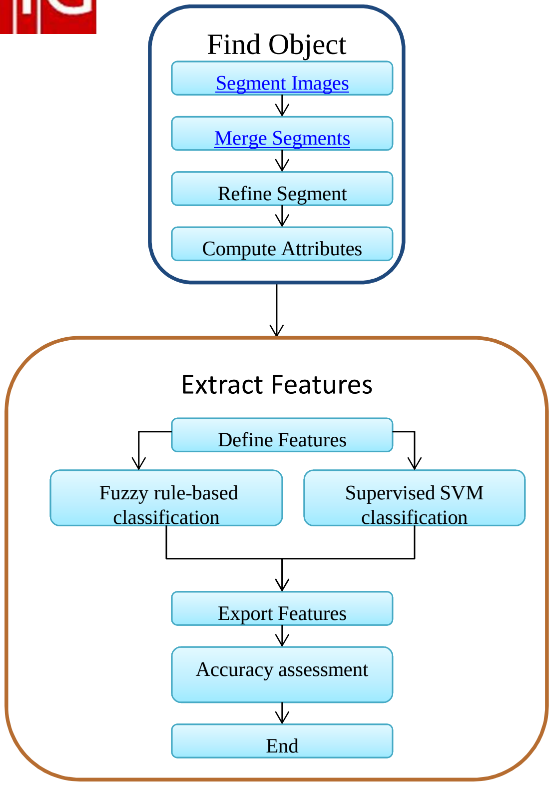

(ENVI-Zoom Tutorial (2010))

Land-cover classes

- **Asbestos roof**
- **Concrete tile roof**
- **Metal roof**
- **Road**
- **Sidewalks**
- **Grass**
- **Trees**
- **Pond**
- **Swimming pool**
- **Shadow**

RBF Kernel was used for SVM classifier. SVM parameters (C and γ) have been optimized using parameter selection technique.(The cross validation determined the optimal parameter **C = 0.5** and **γ = 0.0078 with 5 fold function rate = 99 %**)

Results and Discussions

Supervised SVM object-based classification of LiDAR data and WorldView-2 image

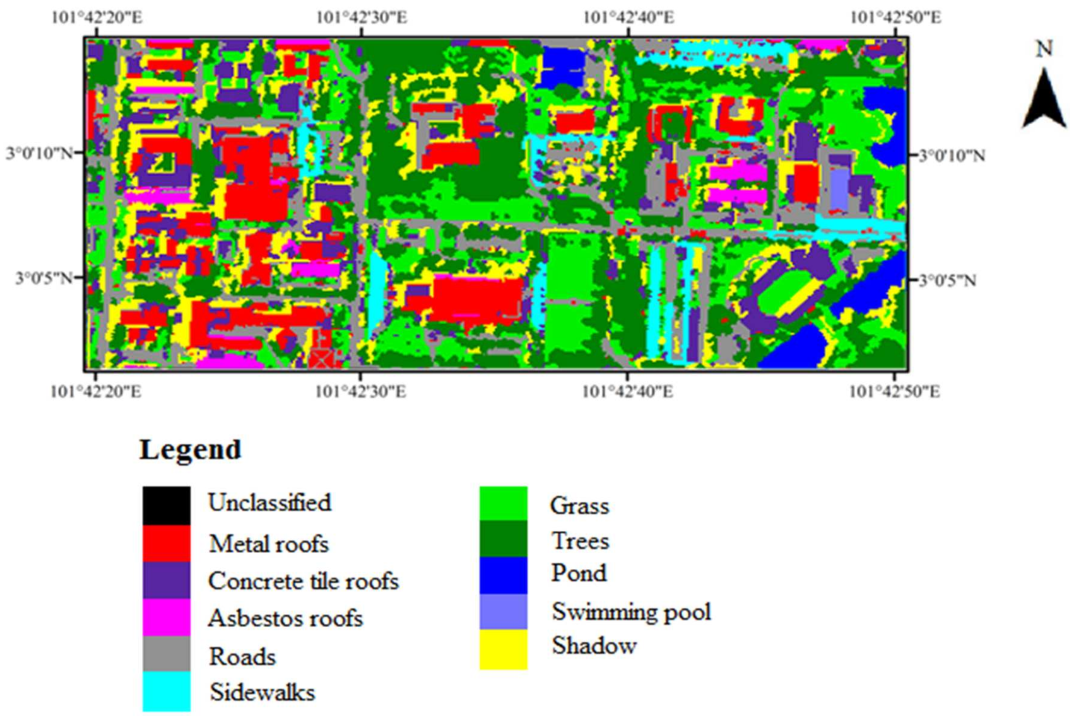

XXV International Federation of Surveyors Congress, Kuala Lumpur, Malaysia, 16 – 21 June 2014

Accuracy assessment of supervised SVM object-based classification

class	Reference total	Classified total	Correct classified	Pa %	Ua %
Mr	80	58	58	72.50	100
Cr	58	57	47	81.03	82.46
Ar	24	40	24	100	60
R	61	43	41	67.21	95.35
S	10	24	10	100	41.67
G	52	52	51	98.08	98.08
T	72	83	71	98.61	85.54
P	33	38	33	100	86.84
Sp	5	5	5	100	100
Sh	39	34	29	74.36	85.29
Overall Accuracy = 85.02%			Kappa Coefficient = 0.82		

Note: Mr =metal roofs, Cr: concrete tile roofs, Ar: asbestos roofs, R= roads, S=sidewalks, G=grass, T=trees, P=pond, Sp= swimming pool, Sh=shadow, Pa= producer accuracy, and Ua= user accuracy

Rule-sets of object-based image analysis

Spatial Attributes

Attribute	Description
AREA	Total area of the polygon, minus the area of the holes. Values are in map units.
LENGTH	The combined length of all boundaries of the polygon, including the boundaries of the holes. This is different than the MAXAXISLEN attribute. Values are in map units.
COMPACT	A shape measure that indicates the compactness of the polygon. A circle is the most compact shape with a value of 1 / pi. The compactness value of a square is 1 / 2(sqrt(pi)). COMPACT = Sqrt (4 * AREA / pi) / outer contour length
CONVEXITY	Polygons are either convex or concave. This attribute measures the convexity of the polygon. The convexity value for a convex polygon with no holes is 1.0, while the value for a concave polygon is less than 1.0. CONVEXITY = length of convex hull / LENGTH
SOLIDITY	A shape measure that compares the area of the polygon to the area of a convex hull surrounding the polygon. The solidity value for a convex polygon with no holes is 1.0, and the value for a concave polygon is less than 1.0. SOLIDITY = AREA / area of convex hull
ROUNDNESS	A shape measure that compares the area of the polygon to the square of the maximum diameter of the polygon. The "maximum diameter" is the length of the major axis of an oriented bounding box enclosing the polygon. The roundness value for a circle is 1, and the value for a square is 4 / pi. ROUNDNESS = 4 * (AREA) / (pi * MAXAXISLEN^2)
FORMFACTOR	A shape measure that compares the area of the polygon to the square of the total perimeter. The form factor value of a circle is 1, and the value of a square is pi / 4. FORMFACTOR = 4 * pi * (AREA) / (total perimeter)^2
ELONGATION	A shape measure that indicates the ratio of the major axis of the polygon to the minor axis of the polygon. The major and minor axes are derived from an oriented bounding box containing the polygon. The elongation value for a square is 1.0, and the value for a rectangle is greater than 1.0. ELONGATION = MAXAXISLEN / MINAXISLEN
RECT_FIT	A shape measure that indicates how well the shape is described by a rectangle. This attribute compares the area of the polygon to the area of the oriented bounding box enclosing the polygon. The rectangular fit value for a rectangle is 1.0, and the value for a non-rectangular shape is less than 1.0. RECT_FIT = AREA / (MAXAXISLEN * MINAXISLEN)

Texture Attributes

Attribute	Description
TX_RANGE	Average data range of the pixels comprising the region inside the kernel. A kernel is an array of pixels used to constrain an operation to a subset of pixels. Refer to the **Texture Kernel Size** preference (see "ENVI Feature Extraction Preferences" on page 60).
TX_MEAN	Average value of the pixels comprising the region inside the kernel.
TX_VARIANCE	Average variance of the pixels comprising the region inside the kernel.
TX_ENTROPY	Average entropy value of the pixels comprising the region inside the kernel. ENVI Zoom computes entropy, in part, from the Max Bins in Histogram preference.

Color Space and Band Ratio Attributes

Attribute	Description
BANDRATIO	Values range from -1.0 to 1.0. See "Band Ratio" on page 30.
HUE	Hue is often used as a color filter and is measured in degrees from 0 to 360. A value of 0 is red, 120 is green, and 240 is blue.
SATURATION	Saturation is often used as a color filter and is measured in floating-point values that range from 0 to 1.0.
INTENSITY	Intensity often provides a better measure of brightness than using the AVGBAND_*x* spectral attribute. Intensity is measured in floating-point values from 0 to 1.0.

Spectral Attributes

Attribute	Description
MINBAND_*x*	Minimum value of the pixels comprising the region in band *x*.
MAXBAND_*x*	Maximum value of the pixels comprising the region in band *x*.
AVGBAND_*x*	Average value of the pixels comprising the region in band *x*.
STDBAND_*x*	Standard deviation value of the pixels comprising the region in band *x*.

(Adapted from ENVI-Zoom Tutorial (2010))

XXV International Federation of Surveyors Congress, Kuala Lumpur, Malaysia, 16 – 21 June 2014

Rule-sets of object-based image analysis

	Land cover classes									
Attribute	MR	CTR	AR	Roads	SDW	Trees	Grass	Lake	SP	SD
stdband6	<0.008	[-0.06, 0.01]			[-0.05, -0.03]					
nDSM	>3.25	>2.41		[-0.28, 2.32]		>1.67	<9.5			
maxband2	1.09									
avgband2	>0.97	<1.12						<0.9	[1.51, 2.68]	
maxband3	>1.32									
avgband4	>0.89	[0.73, 1.49]								
NDVI		[0.66, 1.24]	[0.72, 0.85]							
minband7		[0.72, 1.24]	[0.79, 0.82	[0.59, 0.85]		>0.857	>0.91			
tx_entropy			<0.18			>0.18				
area		>72.29	>161	>113.47	>202.6			>129.07	>10.8 1	
avgband1		[0.87,1 .04]		>0.92						
minband8		>0.35			>0.41					
maindir					<175.76	<0.92				
elongation					>1.33					
tx_mean		<0.06					[0.85, 0.97]			
avgband3							>0.07			
avgband5							<0.98			
avgband8								<0.52	<0.82	
hue								<239.83		
saturation								>0.38		
tx_range										>0.03
avgband7										[0.39, 0.64]
minband1										<0.95

Note: MR= metal roofs, CTR= concrete tile roofs, AR= asbestos roofs, SP= swimming pool, SDW =Sidewalk, and SD= shadows

Rule-based object-based classification of LiDAR data and WorldView-2 image

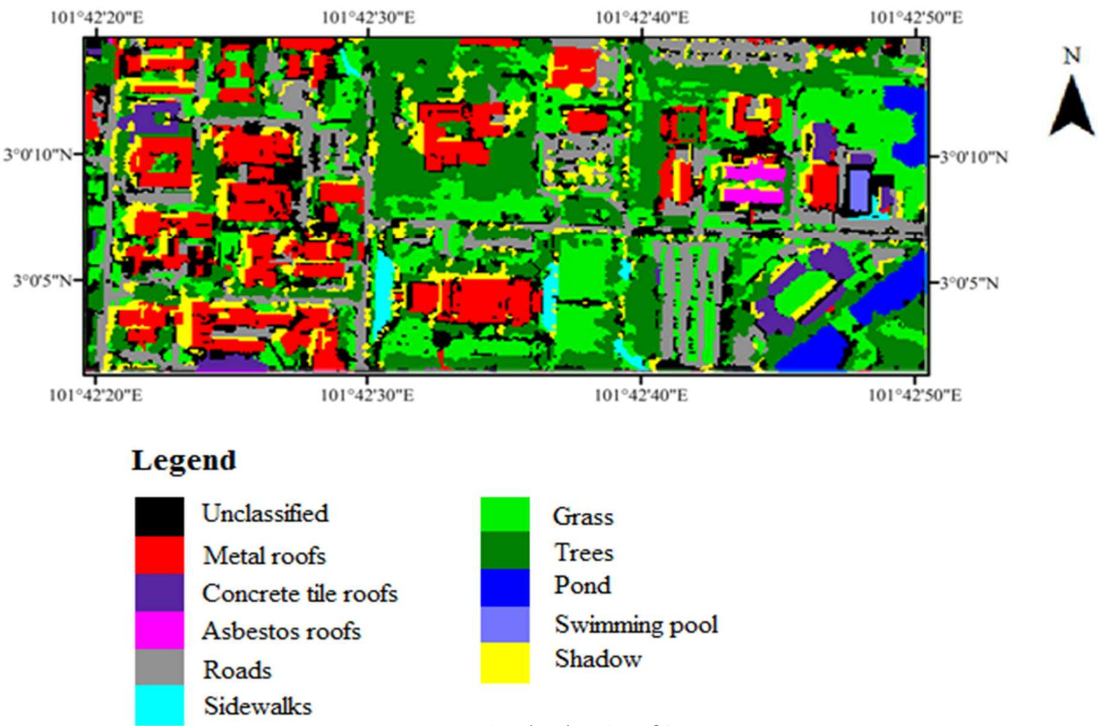

Accuracy assessment of Rule-based object-based classification

class	Reference total	Classified total	Correct classified	Pa %	Ua %
Mr	80	80	78	97.50	97.50
Cr	58	58	52	89.66	100
Ar	24	24	24	100	100
R	61	61	51	83.61	91.07
S	10	10	10	100	100
G	52	52	51	98.08	89.47
T	72	72	71	98.61	92.21
P	33	33	33	100	100
Sp	5	5	5	100	100
Sh	39	39	30	76.92	96.77
Overall Accuracy = 93.07%			Kappa Coefficient = 0.92		

Note: Mr =metal roofs, Cr: concrete tile roofs, Ar: asbestos roofs, R= roads, S=sidewalks, G=grass, T=trees, P=pond, Sp= swimming pool, Sh=shadow, Pa= producer accuracy, and Ua= user accuracy

Conclusion & Recommendations

- Improvement of rule-based classification by nDSM and WorldView-2 data fusion (93.02% overall accuracy)
- Higher accuracy by using the developed rule-sets from spectral, spatial, texture and elevation information
- Effective reduction of misclassifications
- Increase the productivity and efficiency of OBIA

➢ Future study can be done to explore the transferability of established rule-sets.

➢ Expand the work to larger study areas, and explore the performance of different object-based classifiers

References

Arnold Jr, C. L., & Gibbons, C. J. (1996). Impervious surface coverage: the emergence of a key environmental indicator. Journal of the American Planning Association, 62(2), 243-258.

Ballo, S., M. Liu, L. Hou, and J. Chang. 2009. “Pollutants in Storm Water Runoff in Shanghai (China): Implications for Management of Urban Runoff Pollution.” Progress in Natural Science 19 (7): 873–880.

Blaschke, T., Strobl, J., 2001 "What’s wrong with pixels? Some recent developments interfacing remote sensing and GIS."GeoBIT/GIS6, pp. 12-17.

ENVI-Zoom. 2010. ENVI User Guide. Denver, CO: ITT.

F. Frassy, G. Candiani, P. Maianti, A. Marchesi, F. R. Nodari, M. Rusmini, C. Albonico, and M. Gianinetto, "Airborne remote sensing for mapping asbestos roofs in aosta valley", in Geoscience and Remote Sensing Symposium (IGARSS), 2012 IEEE International, A. Moreira and Y.-L. Desnos, Eds., Proc IEEE, 7541-7544 (2012).

Göbel, P., C. Dierkes, and W. Coldewey. 2007. “Storm Water Runoff Concentration Matrix for Urban Areas.” Journal of Contaminant Hydrology 91 (1): 26–42.

Hamedianfar, A., Shafri, H. Z. M., 2013. Development of fuzzy rule-based parameters for urban object-oriented classification using very high resolution imagery. Geocarto International, pp. 1-25. doi: 10.1080/10106049.2012.760006

Hamedianfar, A., Shafri, H. Z. M., Mansor, S., & Ahmad, N. (2014). Improving detailed rule-based feature extraction of urban areas from WorldView-2 image and lidar data. International Journal of Remote Sensing, 35(5), 1876-1899.

Myint, S W., Gober, P., Brazel A, Grossman-Clarke, S., Weng., Q, 2011. Per-pixel vs. object-based classification of urban land cover extraction using high spatial resolution imagery. Remote Sensing of Environment, 115, pp. 1145-1161.

References

Pinho, C. M. D., L. M. G. Fonseca, T. S. Korting, C. M. de Almeida, and H. J. H. Kux. 2012. “Land-Cover Classification of an Intra-Urban Environment Using High-Resolution Images and Object-Based Image Analysis.” International Journal of Remote Sensing 33 (19): 5973–5995.

Safitri Zen, R. Ahamad, K. Gopal Rampal, and W. Omar. 2013 "Use of asbestos building materials in Malaysia: legislative measures, the management, and recommendations for a ban on use". *INT J OCCUP ENV HEAL*. **19**(3), 169-178

Jensen JR. 2005. Introductory digital image processing: a remote sensing perspective. Upper Saddle River (NJ): Prentice Hall.

XXV International Federation of Surveyors Congress, Kuala Lumpur, Malaysia, 16 – 21 June 2014

Acknowledgement

- Financial assistance from Peninsula Malaysia Land Surveyors Board (LJT).
- Financial support from the Ministry of Higher Education(MOHE) Malaysia.

Thank you for your attention!

[1]Department of Civil Engineering, Faculty of Engineering, Universiti Putra Malaysia (UPM)

[2]Geospatial Information Science Research Centre (GISRC), Faculty of Engineering, Universiti Putra Malaysia (UPM)

Email: hzms04@gmail.com

XXV International Federation of Surveyors Congress, Kuala Lumpur, Malaysia, 16 – 21 June 2014